Finite element modelling of carbon fiber - carbon nanostructure - polymer hybrid composite structures

Stelios K. Georgantzinos[1,*], *Stylianos I.* Markolefas[1], *Stamatis A.* Mavrommatis[1], and *Konstantinos P.* Stamoulis[2]
[1]National and Kapodistrian University of Athens, General Department, Greece
[2]Amsterdam University of Applied Sciences, Faculty of Technology, Aviation Academy, Netherlands

Abstract. The present study deals with the numerical modelling of hybrid laminated composites, which can be proved especially useful in the engineering and maintenance of advanced aerospace primary structures. The lamina is comprised of continuous carbon fibers, thermosetting epoxy polymer matrix, as well as carbon nanostructures, such as graphene or carbon nanotubes, inclusions. Halpin-Tsai equations combined with results obtained from nanomechanical analysis are employed in order to evaluate the elastic properties of the carbon nanostructure/polymer matrix. Then, the obtained elastic properties of the hybrid matrix are used to calculate the orthotropic macro-mechanical properties of the unidirectional composite lamina. A hybrid composite plate is modelled as a 2D structure via the utilization of 4-node, quadrilateral, stress/displacement shell finite elements with reduced integration formulation. The convergence and analysis accuracy are tested. The mechanical performance of the hybrid composites is investigated by considering specific configurations and applying appropriate loading and boundary conditions. The results are compared with the corresponding ones found in the open literature, where it is possible.

1 Introduction

The high strength and stiffness, as well as the light weight of the polymer matrix composites make them ideal candidates in numerous automotive, aerospace, medical and other applications. Due to their excellent mechanical performance, carbon nanostructures, such as carbon nanotubes (CNTs) and graphene, can be used to reinforce the polymer matrix of composites, for a further enhancement of their stiffness and strength.

CNTs are cylinders formed by carbon atoms arranged in hexagonal pattern and being covalently bonded with each other through sp^2 hybridization. Their synthesis can be performed through several techniques. Arc evaporation method, laser ablation and chemical vapor deposition are the processes used broadly for production of CNTs [1]. CNTs present exceptional mechanical performance, i.e. remarkably high Young's modulus and strength, as well as low density [2,3].

* Corresponding author: sgeor@uoa.gr

Graphene has a similar carbon atom arrangement as CNTs; however, it is a planar monolayer. It is the thinnest structural material in the world and presents extraordinary mechanical [4,5], electrical [6], optical and chemical properties [7]. One can find various production and processing techniques, as well as potential applications of graphene in [8].

Nowadays, there has been an excessive growth in research associated with the polymer nanocomposites due to development of advanced materials for potential applications [9]. After establishing an increased understanding in the composition – structure – processing – performance dependencies for the class of the composite materials, a great effort has been devoted to enhancing the occasionally unsatisfactory matrix – dominate properties such as the impact damage [10-12]. Graphene or CNTs within the polymer matrix act as fillers which improves the engineering capabilities of a composite. Depending on the interaction between the CNT or graphene and the matrix, mechanical, thermal, magnetic and other properties of the nanocomposite improves substantially [13]. A recent review on polymer nanocomposites and their processing, characterization, and mechanical properties is presented in [14].

Finite Element Method (FEM) is one of the leading approaches for the simulation of physical phenomena and therefore can be straightforwardly used by both academic and industrial groups. Concerning the FEM simulation of the mechanical performance of polymer nanocomposites several works [2,15-17] have been presented in the literature, in which micromechanical analysis is performed. The advantage of the usage of FEM is its efficiency in terms of accuracy and computational effort.

Mehar and Panda [18] examined the deformation of CNT reinforced composite plate, numerically, experimentally and theoretically investigating the role of numerous parameters. They conclude that the bending rigidity increases by adding CNTs to the structure up to 0.2 weight fractions and decreases for higher ones. This phenomenon is explained to agglomeration of carbon nanotubes within the matrix. Hence, it is crucial to develop composite production methods, in which agglomeration does not occur. In an excellent work, Taş and Soykok [19] studied engineering constants of CNT - carbon fiber - polymer hybrid composite lamina and a composite plate configuration using ANSYS, ACP Module. The results have showed that engineering constants increase as the added carbon nanotube fraction is increased.

Beyond the extensive work about the investigation of carbon nanostructures or polymer nanocomposites, there are few studies concerning carbon fiber - carbon nanostructure - polymer hybrid composite structures. In this work, a FEM framework is presented for the analysis and design of hybrid composite laminated structures using conventional 4-node, quadrilateral, stress/displacement shell finite elements with reduced integration formulation. In order to describe the elastic constants of the hybrid composite, Halpin-Tsai equations combined with results obtained from nanomechanical analysis are used for the calculation of the carbon nanostructure/polymer matrix elastic properties and then the corresponding ones of the composite lamina. Assuming a specific plate configuration, the mechanical response of the composite is predicted under different loading conditions.

2 Modelling framework

The finite element modelling framework is based on the combination of the results obtained by mechanical analysis performed in different scales. Starting from the nanoscale, results concerning the elastic constants of CNTs and graphene are selected. Then, the nanoscale results are combined with the macroscale data concerning the polymer material using micromechanical rules, and specifically, here, the Halpin-Tsai model. In this way, the carbon nanostructure/polymer hybrid matrix material elastic constants are predicted. At that time, the mechanical properties of the unidirectional lamina of the hybrid composite can be calculated using the conventional macroscopic models. Therefore, the mechanical

performance of a specific composite can predicted using the classical lamination theory and can be modelled using finite element techniques.

2.1 Calculation of elastic constants

2.1.1 Calculation of size dependent mechanical properties of nanostructures

The elastic mechanical behaviour of different sized carbon nanostructures as graphene and CNTs has been numerically investigated and predicted using a spring-based finite element approach [4, 20]. According to those approaches three-dimensional, two-node, spring-based finite elements of three degrees of freedom per node, are combined in order to model effectively the interatomic interactions presented inside a carbon nanostructure. The calculated variations of mechanical elastic constants have been approached by appropriate size-dependent, non-linear functions of two independent variables, i.e. length and width for graphene, in order to express the analytical rules governing the elastic behaviour. The numerical results have been already validated through comparisons with corresponding data given in the open literature. The significant effect of size and chirality of carbon nanostructures on their elastic behaviour has already been demonstrated.

The Young's modulus $E(w,l)$ in TPa of the graphene can be predicted using the following rational function

$$E_{gr}(w_{gr},l_{gr}) = \frac{P_0+a_{01}w_{gr}+b_{01}l_{gr}+b_{02}{l_{gr}}^2+c_{02}w_{gr}l_{gr}}{1+a_1w_{gr}+b_1l_{gr}+a_2{w_{gr}}^2+b_2{l_{gr}}^2+c_2w_{gr}l_{gr}},\ 0<w_{gr},l_{gr}\leq 10\text{ nm}, \quad (1)$$

where $P_0, a_{01}, b_{01}, b_{02}, c_{02}, a_1, b_1, a_2, b_2,$ and c_2 are constants, which are determined by non-linear fitting, while w_{gr} and l_{gr} are the graphene width and length, respectively. The values of the constants of Equation (1) concerning both the two chirality directions of graphene are presented in Table 1. The accuracy of this equation compared with the finite element predictions and expressed by the coefficient of determination is calculated to be over 99.5%.

Table 1. Fitting parameters of Equation (1) for the prediction of Young's modulus variation in TPa.

Direction	P_0	a_{01}	b_{01}	b_{02}	c_{02}	a_1	b_1	a_2	b_2	c_2
Zig zag	676	13640	-2532	58250	19170	11760	-4.7E-4	63.72	85900	17870
Armchair	2.98	3.03	13.55	0.893	-1.197	3.042	19.53	1.148E-1	1.225	-1.634

2.1.2 Calculation of hybrid matrix elastic constants

Halpin-Tsai model proposed for discontinuous fiber reinforced lamina is employed to calculate the Young's modulus of the carbon nanotube/polymer matrix system. In this model, carbon nanotubes are considered as long randomly oriented discontinuous fibers. Young's modulus of the carbon nanotube-added matrix can be calculated from the following equation [19]:

$$E_{m-cnt} = \frac{3}{8}\frac{1+2\left(\frac{l_{nt}}{d_{NT}}\right)\left(\frac{\left(\frac{E_{eq}}{E_m}\right)-1}{\left(\frac{E_{eq}}{E_m}\right)+2\left(\frac{l_{nt}}{d_{NT}}\right)}\right)V_{nt}}{1-\left(\frac{\left(\frac{E_{eq}}{E_m}\right)-1}{\left(\frac{E_{eq}}{E_m}\right)+2\left(\frac{l_{nt}}{d_{NT}}\right)}\right)V_{nt}}E_m + \frac{5}{8}\frac{1+2\left(\frac{\left(\frac{E_{eq}}{E_m}\right)-1}{\left(\frac{E_{eq}}{E_m}\right)+2}\right)V_{nt}}{1-\left(\frac{\left(\frac{E_{eq}}{E_m}\right)-1}{\left(\frac{E_{eq}}{E_m}\right)+2}\right)V_{nt}}E_m\,, \tag{2}$$

where E_m is Young's modulus of matrix, V_{NT} is volume content of carbon nanotube and l_{NT} and d_{NT} are length and diameter of carbon nanotube, respectively. E_{eq} is equivalent modulus of the nanotube considering the hollow tube as a solid cylinder and can be expressed as

$$E_{eq} = \left(\frac{2t}{r}\right)E_{NT}, \tag{3}$$

where t, r, and E_{NT} are wall thickness, radius and Young's modulus of nanotube, respectively. Following equation developed by Tsai and Pagano can be used to calculate the shear modulus of the carbon nanotube-added matrix [19].

$$G_{m-cnt} = \frac{1}{8}\frac{1+2\left(\frac{l_{nt}}{d_{nt}}\right)\left(\frac{\left(\frac{E_{eq}}{E_m}\right)-1}{\left(\frac{E_{eq}}{E_m}\right)+2\left(\frac{l_{nt}}{d_{nt}}\right)}\right)V_{nt}}{1-\left(\frac{\left(\frac{E_{eq}}{E_m}\right)-1}{\left(\frac{E_{eq}}{E_m}\right)+2\left(\frac{l_{nt}}{d_{nt}}\right)}\right)V_{nt}}E_m + \frac{1}{4}\frac{1+2\left(\frac{\left(\frac{E_{eq}}{E_m}\right)-1}{\left(\frac{E_{eq}}{E_m}\right)+2}\right)V_{nt}}{1-\left(\frac{\left(\frac{E_{eq}}{E_m}\right)-1}{\left(\frac{E_{eq}}{E_m}\right)+2}\right)V_{nt}}E_m, \tag{4}$$

The Poisson's ratio for carbon nanotube-added matrix presenting exhibiting quasi-isotropic behaviour can be predicted from following equation

$$\nu_{m-cnt} = \frac{E_{m-cnt}}{2G_{m-cnt}} - 1. \tag{5}$$

Considering the mechanical response of the graphene/polymer matrix and assuming that the dimension of graphene inclusion is limited in nanoscale, the three dimensional (3D) Halpin-Tsai model for randomly oriented discontinuous rectangular reinforcements can be employed. According to this model, the Young's modulus of the graphene/polymer matrix can be predicted by the following equation

$$E_{m-gr(3D)} = \frac{1}{5}E_L + \frac{4}{5}E_T \tag{6}$$

where

$$E_L = \frac{1+\xi_L\eta_L V_{gr}}{1-\eta_L V_{gr}}E_m, \tag{7}$$

$$E_T = \frac{1+\xi_T\eta_T V_{gr}}{1-\eta_T V_{gr}}E_m, \tag{8}$$

and

$$\eta_L = \frac{\frac{E_{gr}}{E_m}-1}{\frac{E_{gr}}{E_m}+\xi_L}E_m,\ \eta_T = \frac{\frac{E_{gr}}{E_m}-1}{\frac{E_{gr}}{E_m}+\xi_T}E_m\,. \tag{9}$$

$$\xi_L = 2\frac{l_{gr}}{t_{gr}} + 40{V_{gr}}^{10}, \xi_T = 2\frac{w_{gr}}{t_{gr}} + 40{V_{gr}}^{10}, \tag{10}$$

while V_{gr} is the volume fraction of graphene in the polymer matrix.

Adopting the two-dimensional (2D) Halpin-Tsai model for randomly oriented discontinuous rectangular reinforcements, Young's and shear moduli can be calculated through the following equations

$$E_{m-gr(2D)} = \frac{3}{8}E_L + \frac{5}{8}E_T, \tag{11}$$

$$G_{m-gr(2D)} = \frac{1}{8}E_L + \frac{1}{4}E_T. \tag{12}$$

Assuming that Poisson's ratio for both 2D and 3D Halpin-Tsai models are approximately similar, it is calculated that

$$v_{m-gr} = v_{m-gr}(3D) = \frac{E_{m-gr(2D)}}{2G_{m-gr(2D)}} - 1. \tag{13}$$

Therefore, the shear modulus of the graphene/polymer matrix that exhibits quasi-isotropic behaviour can be calculated from the following equation

$$G_{m-gr(3D)} = \frac{E_{m-gr(3D)}}{2(v_{m-gr}+1)}. \tag{14}$$

2.1.3 Calculation of elastic constants of hybrid composite lamina

Young's modulus of a unidirectional lamina in longitudinal direction, E_1, and Poisson's ratio, v_{12} can be calculated by utilizing the standard rule of mixture [21] as following

$$E_1 = E_f V_f + E_{m-cn}V_m, \tag{15}$$

$$v_{12} = v_f V_f + v_{m-cn}V_m, \tag{16}$$

where E_f, V_f, v_f and V_m are Young's modulus of fiber, volume fraction of fiber, Poisson's ratio of fiber and volume fraction of matrix, respectively, while $E_{m-cn} = E_{m-cnt}$ or E_{m-gr} and $v_{m-cn} = v_{m-cnt}$ or v_{m-gr}. The remaining orthotropic material properties, i.e. Young's modulus in transverse direction, E_2, Poisson's ratio, v_{23} and shear moduli, G_{12} and G_{23} are calculated by the following Halpin-Tsai [22] equation

$$\frac{P}{P_m} = \frac{1+\xi\eta V_f}{1-\eta V_f}, \tag{17}$$

where P_m is the related properties of carbon nanostructure/polymer matrix. Moreover, η is an experimental factor, which is calculated by using following expression

$$\eta = \frac{\frac{P_f}{P_m}-1}{\frac{P_f}{P_m}+\xi}, \tag{18}$$

where P_f and P_m are the related properties of fiber and carbon nanostructure/polymer matrix, respectively. Note that ξ is a measure of reinforcement geometry which depends on loading conditions. ξ is chosen as 2 for calculation of E_2 and as 1 for calculations of v_{23}, G_{12} and G_{23}.

2.2 Finite element modelling of a composite structure

Shell elements allow for modelling thin to moderately thick shells, down to a side-to-thickness ratio of 10. The Abaqus FEM program S4R conventional shell element is a 4-node, quadrilateral, stress/displacement shell element with reduced integration and a large-strain formulation. These elements are thick shell elements (non-zero transverse shear deformation) enforcing the first-order shear deformation theory (FSDT).

The first assumption of FSDT is that a straight line drawn through the thickness of the shell in the undeformed configuration may rotate but it will remain straight when the shell deforms. The second one is that the change of the shell thickness is negligible as the shell deforms. These assumptions are verified by experimental observation in most laminated shells when the ratio between the shortest surface dimension and the thickness, is larger than 10, as well as the stiffness of the laminae in shell material coordinates does not differ by more than two orders of magnitude.

Obtaining the elastic constants of the composite lamina and knowing the actual laminate stacking sequence (LSS) of a specific configuration, the laminate properties can be computed. A representative example of a finite element model is presented in Figure 1.

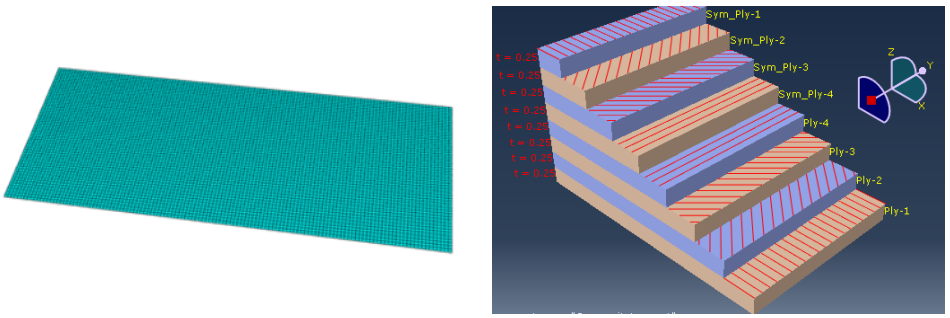

(a) (b)

Figure. 1. (a) Finite element model of a composite plate, and (b) LSS.

3 Results and discussion

In order to test the performance of the proposed method the following cases are considered. CNTs used in the model have l_{NT} = 20000 nm, d_{NT} = 20 nm, wall thickness t_{NT} =1.5 nm, and E_{NT} = 450000 MPa [23]. Graphene configuration and properties are described by w_{gr} = 10.02 nm, l_{gr} = 9.97 nm, and E_{gr} = 735000 MPa. Material properties of carbon fibers are E_{f11} = 230000 MPa, E_{f22} = 15410 MPa, v_{f23} = 0.46, v_{f12} = 0.29, G_{f12} = 10040 MPa, and G_{f23} = 10040 MPa [19]. Matrix material is assumed to be a polyester resin with E_m = 3000 MPa, G_m = 1139.8 MPa, and v_m = 0.316. Volume fraction of fiber and matrix is determined to be 60% and 40%, respectively.

Table 2. Material properties of the hybrid composite lamina with CNTs inclusions.

		CNT inclusion		Graphene inclusion	
V_{CN} (vol%)	0	0.2	0.5	0.2	0.5
E_1 (MPa)	139200	143610	150972	153000	187600
E_2 (MPa)	7799	14485	21450	23100	50250
G_{12} (MPa)	3194	7440	10514	11497	20560
G_{23} (MPa)	2560	5123	7254	8042	16449
v_{12}	0.307	0.348	0.350	0.3073	0.307

		CNT inclusion		Graphene inclusion	
v_{23}	0.404	0.450	0.452	0.4040	0.404

Material properties of the hybrid composite lamina with CNTs or graphene inclusions, calculated according to the proposed method are presented in Table 2. As expected, the hybrid composite with graphene inclusions exhibits better mechanical properties compared to CNTs inclusions because of the higher mechanical performance of graphene. Furthermore, graphene is a 2D structure and, thus, offers its advantages in two directions rather than the single direction of CNTs.

Table 3. Maximum bending deflection (mm) under different boundary conditions.

		CNT inclusion			Graphene inclusion
	Volume fraction	FEM (Present)	Theoretical [16]	FEM [16]	FEM (Present)
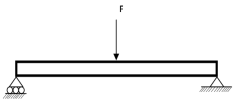	0	0.972	0.964	1.026	0.972
	0.2	0.865	0.860	0.918	0.774
	0.5	0.792	0.795	0.837	0.598
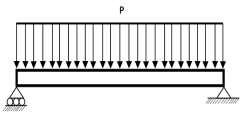	0	0.376	0.401	0.410	0.376
	0.2	0.345	0.362	0.367	0.324
	0.5	0.320	0.332	0.334	0.249

According to the ASTM D7264 standard, a $64 \times 25 \times 2$ mm^3 composite plate is modelled. The plate is comprised of 8 unidirectional layers, possessing the mechanical properties computed in Table 2. The stacking sequence of the composite under consideration is [0/+45/-45/90]*s* (Figure 1b). The model has been tested for its convergence in terms of mesh density and the mesh depicted in Figure 1a is finally chosen. The hybrid composite plates of different carbon nanostructure inclusion types and volume fractions are subjected to bending loading ($F = 250$ N, $P = 0.1$ MPa). The analysis results obtained by the present method are compared with corresponding ones found in the literature in Table 3. A good agreement between the different methods is observed. To the author's best knowledge, numerical results concerning carbon fiber – graphene – polymer composites are presented for first time. Composite structures with graphene inclusions seem to present better mechanical performance than the ones with CNTs inclusions.

In Figure 2, the distribution of the bending deflection (for some cases of Table 3) are depicted.

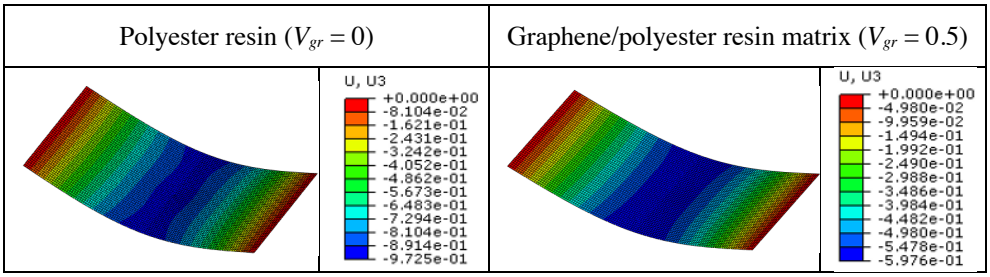

Figure. 2. Deformed mesh and deflection distribution of composite plates (F = 250 N).

4 Conclusions

A modelling framework for the simulation of the mechanical behaviour of carbon fiber - carbon nanostructure - polymer hybrid composite structures was presented. The proposed method can reveal the potential for the improvement of the mechanical performance of composite structures using carbon nanostructure inclusions. The stiffness of structures increases significantly due to the presence of nanostructures and graphene inclusion hybrid laminates demonstrate better mechanical performance compared to CNT hybrid laminates.

References

1. L.S. Ying, M.A.M. Salleh, H.B.M. Yusoff, S.B.A. Rashid, J.B.A. Razak, J. Ind. Eng. Chem. **17**, 367 (2013)
2. S.K. Georgantzinos, G.I. Giannopoulos, N.K. Anifantis, J. Comput. Theor. Nanos. **7**, 1436 (2010)
3. G.I. Giannopoulos, A.P. Tsiros, S.K. Georgantzinos, Mech. Adv. Mater. Struc. **20**, 730 (2013)
4. S.K. Georgantzinos, J. Comput. Theor. Nanos. **14**, 5347 (2017)
5. S.K. Georgantzinos, G.I. Giannopoulos, N.K. Anifantis, Proc. Inst. Mech. Eng. N J. Nanoeng. Nanosyst. **224**, 163 (2010)
6. S.K. Georgantzinos, G.I. Giannopoulos, A. Fatsis, N.V. Vlachakis, Physica E **84**, 27 (2016)
7. J.R. Potts, D.R. Dreyer, C.W. Bielawski, R.S. Ruoff, Polymer **52**, 5 (2011)
8. G. Mittal, V. Dhand, K.Y. Rhee, S.J. Park, W.R. Lee, J. Ind. Eng. Chem. **21**, 11 (2015)
9. P.M. Ajayan, O. Stephan, C. Colliex, D. Trauth, Science **265**, 1212 (1994)
10. K. Stamoulis, S.K. Georgantzinos, G.I. Giannopoulos, Int. J. Struct. Integr. https://doi.org/10.1108/IJSI-10-2018-0063 (2019)
11. 11. P. Dimoka, S. Psarras, C. Kostagiannakopoulou, V. Kostopoulos, Materials **12**, 1080 (2019)
12. 12. E. Giannaros, A. Kotzakolios, G. Sotiriadis, S. Tsantzalis, V. Kostopoulos. Compos. Struct. **204**, 745 (2018)
13. R.K. Layek, A.K. Nandi, Polymer **54**, 5087 (2013).
14. S. Fu, Z. Sun, P. Huang, Y. Li, N. Hu, Nano Mater. Sci. **1**, 2 (2019)
15. G.I. Giannopoulos, S.K. Georgantzinos, D.E. Katsareas, N.K. Anifantis, Comput. Model. Eng. Sci. **56**, 231 (2010)

16. A. Dabbagh, A. Rastgoo, F. Ebrahimi, Thin Wall Struct. **140**, 304 (2019)
17. G.I. Giannopoulos, S.K. Georgantzinos, P.A. Kakavas, N.K. Anifantis, Fuller. Nanotub. Car. N. **21**, 248 (2013)
18. K. Mehar, S.K. Panda, Adv. Polym. Tech. **37**, 1643 (2018)
19. H. Taş, I.F. Soykok, Compos. Part B-Eng. **159**, 44 (2019)
20. G.I. Giannopoulos, I.A. Liosatos, A.K. Moukanidis, Physica E **44**, 124 (2011)
21. R. M. Jones, *Mechanics of composite materials* (CRC press, 2014)
22. J.C. Halpin, J.L. Kardos, Polym. Eng. Sci. **16**, 344 (1976)
23. M.A. Rafiee, J. Rafiee, Z. Wang, H. Song, Z.Z. Yu, N. Koratkar, ACS Nano **3**, 3884 (2009)